

Role of Crystalline Structure in Allyl Alcohol Selective Oxidation over Mo_3VO_x Complex Metal Oxide Catalysts

Toru Murayama,^{*,[a, b]} Benjamin Katryniok,^[c, d] Svetlana Heyte,^[c] Marcia Araque,^[c, d] Satoshi Ishikawa,^[a, f] Franck Dumeignil,^[c, e] Sébastien Paul,^[c, d] and Wataru Ueda^[a, f]

The role of the crystalline phase of Mo_3VO_x in the catalytic oxidation of allyl alcohol over four kinds of crystalline (orthorhombic, trigonal, tetragonal, amorphous) Mo_3VO_x catalysts was investigated to determine the active sites for the reactions. Tetragonal Mo_3VO_x was found less active for the formation of acrylic acid from allyl alcohol, although acrolein was obtained selectively at higher temperature. For orthorhombic and trigonal Mo_3VO_x catalyst, allyl alcohol converted to acrolein and

propanal competitively at the mouth of the heptagonal channel over the a - b plane of the rod-type crystalline particles, and these aldehydes were oxidized consecutively to acrylic acid. Acrylic acid was formed effectively at increased reaction temperature over orthorhombic, trigonal and amorphous Mo_3VO_x catalysts, and the maximum yields of acrylic acid were 73% for the orthorhombic Mo_3VO_x catalyst and 72% for the trigonal Mo_3VO_x catalyst at 350 °C.

Introduction

The use of glycerol as a starting material for obtaining commodity chemicals has gained much attention.^[1-4] Especially, the oxidative dehydrogenation of glycerol to acrylic acid has become into the focus, because the latter is a widely used monomer for the synthesis of resins and superabsorbents. However, the direct synthesis of acrylic acid from glycerol is challenging,^[5,6] whereby improvement of the synthesis route through two-step conversion is more favourable. The first step consists in dehydration of glycerol to acrolein and the second step in the oxidation of acrolein to acrylic acid. In any case, allyl intermediate products are important to understand the mechanism. According to this background, we have focused on allyl alco-

hol as an intermediate product.^[7-12] Nowadays, allyl alcohol is conventionally obtained from acrolein by selective hydrogenation or from propylene oxide^[13] by using a lithium phosphate catalyst.^[14] Nevertheless, it can also be obtained from renewable sources such as glycerol^[15-17] or propanediol.^[18] Thus, the oxidation of allyl alcohol is a promising way for a sustainable synthesis of acrylic acid. At the current state, there are only a few reports on the selective oxidation of allyl alcohol to acrylic acid.^[19,20] National Distillers and Chemical Corporation reported in 1977 a Pd-Cu/ Al_2O_3 catalyst giving 80% conversion of allyl alcohol and 23% selectivity to acrylic acid. Nippon Shokubai claimed a Mo-V-W-Cu-Zr complex oxide yielding 59.5% acrylic acid from allyl alcohol.

Previously, we have reported a method for the synthesis of four kinds of crystalline (orthorhombic, trigonal, tetragonal and amorphous) Mo_3VO_x and their reactivity for selective oxidation of light alkanes^[21] and acrolein.^[22,23] These four kinds of Mo_3VO_x materials possess similar chemical compositions with the same layer-type structure in the c direction and a long-rod shaped crystal (Figure 1). The overall crystal structure is determined by the network arrangement of pentagonal $\{\text{Mo}_6\text{O}_{21}\}$ units in the a - b plane. The arrangement of the a - b plane of amorphous

[a] Prof. Dr. T. Murayama, Dr. S. Ishikawa, Prof. Dr. W. Ueda
Institute for Catalysis
Hokkaido University
N-21 W-10, Sapporo 001-0021 (Japan)
E-mail: murayama@tmu.ac.jp

[b] Prof. Dr. T. Murayama
Research Center for Gold Chemistry
Tokyo Metropolitan University
1-1 Minami-Osawa, Hachioji, Tokyo 192-0397 (Japan)

[c] Dr. B. Katryniok, Dr. S. Heyte, Dr. M. Araque, Prof. Dr. F. Dumeignil,
Prof. Dr. S. Paul
Unité de Catalyse et Chimie du Solide
UCCS (UMR CNRS 8181)
Cit  Scientifique, Villeneuve d'Ascq (France)

[d] Dr. B. Katryniok, Dr. M. Araque, Prof. Dr. S. Paul
Ecole Centrale de Lille, ECLille,
Villeneuve d'Ascq (France)

[e] Prof. Dr. F. Dumeignil
University of Lille
Villeneuve d'Ascq (France)

[f] Dr. S. Ishikawa, Prof. Dr. W. Ueda
Kanagawa University
Rokkakubashi, Kanagawa-ku, Yokohama (Japan)

Supporting information for this article can be found under <http://dx.doi.org/10.1002/cctc.201600430>.

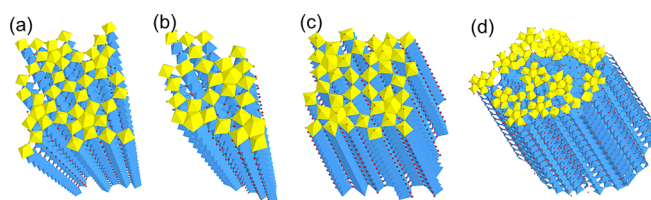


Figure 1. Structure models of a) orthorhombic, b) trigonal, c) tetragonal and d) amorphous Mo_3VO_x . (Yellow polyhedron: M-O octahedron (M=Mo, V) located on the surface, blue polyhedron: M-O octahedron (M=Mo, V) and red dot: oxygen.)

Mo_3VO_x (Figure 1d) is an interconnection of the crystal structure motifs of $\{\text{Mo}_6\text{O}_{21}\}$ units and micropore channels but without long-range order. This layer-type Mo_3VO_x is denoted as amorphous Mo_3VO_x in this report. Orthorhombic, trigonal and amorphous Mo_3VO_x materials are classified into similar structure-type groups, but tetragonal Mo_3VO_x is excluded because the former materials contain empty heptagonal channels, whereas the latter does not. Among these catalysts, Mo_3VO_x catalysts exhibiting heptagonal channels in the structure showed good catalytic activity in acrolein oxidation, whereas no catalytic activity was observed for catalysts without heptagonal channels in the structure,^[24] indicating that the heptagonal channels of Mo_3VO_x are responsible for activating acrolein.

In this study, we investigated the effect of the crystalline structure on selective oxidation of allyl alcohol to acrylic acid. This is the first report on allyl alcohol selective oxidation using crystalline Mo_3VO_x complex metal oxides. Furthermore the influence of the reaction conditions was examined.

Results and Discussion

Four kinds of crystalline (orthorhombic, trigonal, amorphous, tetragonal) Mo_3VO_x catalysts were synthesized and tested for allyl alcohol oxidation. Table S1 in the Supporting Information summarizes the results of characterization of crystalline Mo_3VO_x catalysts. Chemical compositions of the catalysts were found to be almost the same and the ratios of V/Mo were in the range of 0.32–0.37. The external surface areas calculated by the *t*-plot method were in the range from 2.7 to 12.4 m^2g^{-1} .

In Figure 2 the XRD patterns of the four catalysts are shown before and after the reaction at 350 °C for 12 h. A silicon non-reflective sample holder was used for the catalysts after the re-

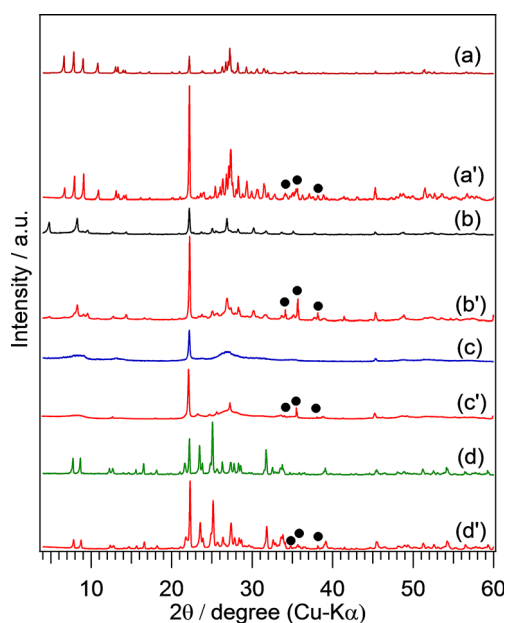


Figure 2. XRD patterns a) orthorhombic, b) trigonal, c) amorphous and d) tetragonal Mo_3VO_x catalysts before and after allyl alcohol oxidation (a', b', c', d'). (Diffraction peaks of SiC from catalyst dilution are shown as ●.)

action because of the small amount of samples. No other diffraction peaks based on impurities were observed for the used catalyst than the diffraction peaks of SiC, which was used as a diluent. The rod-shape morphology of crystalline Mo_3VO_x catalysts was maintained after the tests (Figure 3). Characteristic

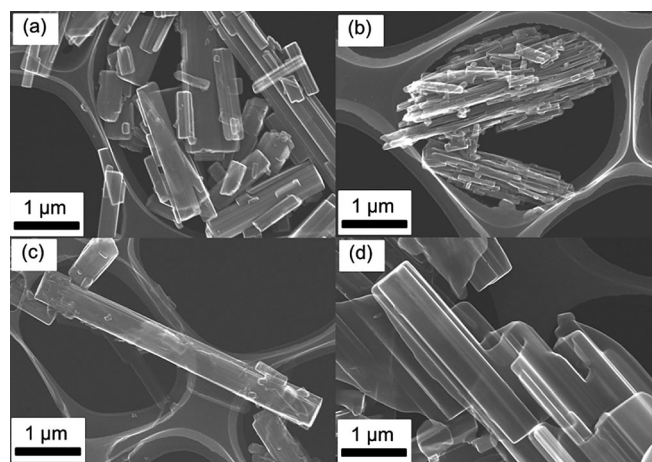


Figure 3. STEM images of a) orthorhombic, b) trigonal, c) amorphous and d) tetragonal Mo_3VO_x catalysts after allyl alcohol oxidation reaction.

diffraction peaks corresponding to each crystalline phase were observed at the low-angle region of less than $2\theta = 10^\circ$. Diffraction peaks at $2\theta = 22.2^\circ$ and 45.3° were observed for all samples, indicating that the materials are all of an octahedron-based layered-type structure with a layer lattice distance of approximately 0.4 nm (Table S1). The amorphous Mo_3VO_x catalyst gave a very broad peak at the low-angle region, indicating that the material—as expected—is not well crystallized in the *a*–*b* plane.^[24]

The catalytic oxidation of allyl alcohol to acrylic acid was performed over the four different Mo_3VO_x catalysts, and their catalytic performances as a function of the reaction temperature are shown in Figure 4. The products detected were acrylic acid, propionic acid, acetic acid, propanal, acrolein, acetaldehyde, acetone, CO and CO_2 . Among these products, the yields in acetaldehyde and acetone were less than 0.5% unless otherwise noted, whereby the results for acetaldehyde and acetone were omitted from the figures. Surprisingly, some hydrogenated products including propanal and propionic acid were found as by-products in the case of allyl alcohol oxidation, which is generally not the case in acrolein oxidation (Scheme 1). From the results one can see that—as expected—the allyl alcohol conversion increased with the reaction temperature over all catalysts. Orthorhombic Mo_3VO_x and trigonal Mo_3VO_x catalysts showed almost the same behaviour, reaching full conversion at 275 °C. Over these two catalysts, propanal and acrolein were obtained as main products at low temperature ($\leq 200^\circ\text{C}$, Table 1). The selectivity in these two products decreased gradually with increase in reaction temperature giving rise to acrylic acid and propionic acid yielding 66% acrylic acid at 350 °C for the orthorhombic Mo_3VO_x catalyst and 68% at 325 °C for the trigonal Mo_3VO_x catalyst. A further increase in the reaction

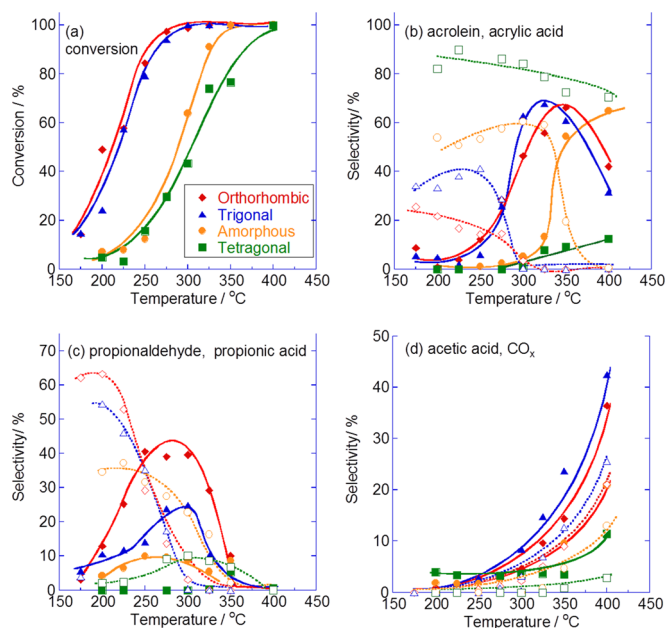
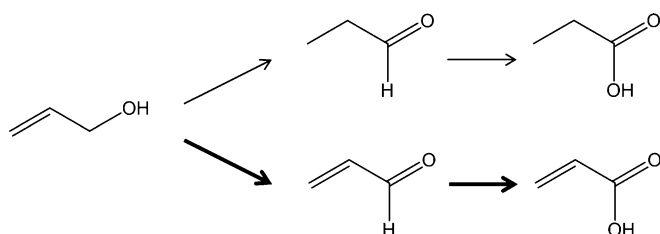


Figure 4. Conversion and selectivity changes as a function of reaction temperature in selective oxidation of allyl alcohol over orthorhombic Mo_3VO_x (\blacklozenge , \blacktriangleright), trigonal Mo_3VO_x (\blacktriangle , \blacktriangleleft), tetragonal Mo_3VO_x (\blacksquare , \blacktriangleright), and amorphous Mo_3VO_x (\bullet , \circ) catalysts. a) Allyl alcohol conversion and selectivities to b) acrolein (open symbols and dashed lines) and acrylic acid (filled symbols and solid lines), c) propanal (open symbols and dashed lines) and propionic acid (filled symbols and solid lines), and d) acetic acid (open symbols and dashed line) and CO_x (filled symbols and solid lines). Reaction conditions: Catalyst 50 mg, 2 bar, allyl alcohol/ O_2 / H_2O / $(\text{N}_2 + \text{He}) = 0.7:1.5:29.5:8.3 \text{ mL min}^{-1}$.



Scheme 1. Oxidation of allyl alcohol to acrylic acid.

| Catalyst | Reaction Temp. [°C] | Conv. [%] | Selectivity [%] | | | | |
|---------------------------------------|---------------------|-----------|-----------------|----------|----------------|----------|---------------|
| | | | Acrylic acid | Acrolein | Propionic Acid | Propanal | CO_x |
| Orthorhombic Mo_3VO_x | 200 | 49 | 1.0 | 21.7 | 12.9 | 63.3 | 0.9 |
| Trigonal Mo_3VO_x | 200 | 46 | 1.4 | 33.6 | 11.4 | 52.2 | 1.3 |
| Tetragonal Mo_3VO_x | 200 | 4.8 | 0 | 82.1 | 0 | 2.2 | 4.0 |
| Amorphous Mo_3VO_x | 200 | 7.1 | 0 | 53.9 | 4.2 | 34.6 | 1.9 |

[a] Reaction conditions: catalyst 50 mg, 2 bar, allyl alcohol/ O_2 / H_2O / $(\text{N}_2 + \text{He}) = 1:2.2:42.1:11.8$ (total flow rate of 40 mL min^{-1}), contact time = $0.00125 \text{ g}_{\text{cat}} \text{ min mL}^{-1}$.

temperature favoured the formation of CO_x and acetic acid. The conversion of oxygen reached 100% at 400 °C. Notably, the catalysts showed stable oxidation activity (Figure S1, Supporting Information) under stream (12 h).

Compared to the orthorhombic Mo_3VO_x and trigonal Mo_3VO_x catalysts, the conversion of allyl alcohol over the tetragonal Mo_3VO_x catalyst was far less. Furthermore, the distribution of obtained products was totally different, and the main product was acrolein with a selectivity of approximately 80%. These results clearly suggest that the tetragonal Mo_3VO_x catalyst contains active sites for the conversion of allyl alcohol to acrolein, but these active sites are different from those for the oxidation of acrolein to acrylic acid. Moreover, the active sites for the conversion of allyl alcohol to acrolein are clearly less active because the conversion of allyl alcohol was lower than that of the other crystalline Mo_3VO_x catalyst.

Finally, the amorphous Mo_3VO_x catalyst also showed less activity than the orthorhombic Mo_3VO_x and trigonal Mo_3VO_x catalysts. Unlike these catalysts, the selectivity to acrolein was higher than that to propanal at a lower temperature.

These results strongly suggest that the oxidation of allyl alcohol to acrylic acid includes the consecutive oxidation of acrolein. Therefore space velocity is an important factor. In Figure S2, the conversion of allyl alcohol and selectivities to acrylic acid, propionic acid, acetic acid, propanal, acrolein and CO_x are shown under the condition of various contact times and reaction temperatures over the four Mo_3VO_x catalysts. The catalyst weight was adjusted to 0.050, 0.025 and 0.100 g and total flow rates of reactant gas were adjusted to 20, 40, 60 and 80 mL min^{-1} with the same gas composition.

As expected, the conversion of allyl alcohol over orthorhombic Mo_3VO_x catalysts at 250 °C increased with increase in contact time (Figure S2, I–250 °C). The selectivities to propionic acid and acrylic acid increased at the same time detrimental to the selectivity in propanal and acrolein, suggesting that intermediately formed propanal and acrolein were consecutively oxidized to propionic acid and acrylic acid as depicted in Scheme 1. The yield of propionic acid was 75% for a weight-flow ratio (W/F) between 3.8 and $5.0 \times 10^{-3} \text{ g}_{\text{cat}} \text{ min mL}^{-1}$ and that of acrylic acid was 20% in the same range. Almost the same behaviour was observed over orthorhombic Mo_3VO_x catalysts at 300 °C (Figure S2, I–300 °C). However, the selectivity to acrylic products (acrolein and acrylic acid) was higher than at 250 °C. At a contact time above $W/F = 2.5 \times 10^{-3} \text{ g}_{\text{cat}} \text{ min mL}^{-1}$, the acrylic acid and propionic acid yield decreased owing to the consecutive oxidation to CO_x . At 350 °C, the conversion of allyl alcohol reached 100% at $W/F = 0.3 \times 10^{-3} \text{ g}_{\text{cat}} \text{ min mL}^{-1}$ and the yield for propionic acid was much less than that at 300 °C (Figure S2, I–300 °C). The maximum yield in acrylic acid (73%) was obtained at $0.3 \times 10^{-3} \text{ g}_{\text{cat}} \text{ min mL}^{-1}$. In Figure S2 (I–400 °C) the results at 400 °C are shown, indicating that the yield of acrylic acid was still obtained but that the consecutive oxidation to CO_x was promoted.

Over the trigonal Mo_3VO_x catalyst, the trend was the same as for the orthorhombic Mo_3VO_x catalyst except for the distribution of products (Figure S2, II). The selectivity to hydrogenated products was suppressed at a lower reaction temperature.

The maximum yield in acrylic acid was 72% at 350 °C and $W/F = 0.3 \times 10^{-3} \text{ g}_{\text{cat}} \text{ min mL}^{-1}$ over the trigonal Mo_3VO_x catalyst.

The tetragonal Mo_3VO_x catalyst was again less active than the orthorhombic Mo_3VO_x and trigonal Mo_3VO_x catalysts for the oxidation of allyl alcohol. Over the tetragonal Mo_3VO_x catalysts, the conversion of allyl alcohol increased with increase in contact time, whereas the selectivity to acrolein was unchanged (80%) regardless of the contact time at 250 °C and 300 °C (Figure S2, III–250 °C, –300 °C). At 350 °C, the conversion of allyl alcohol reached 100% (for $W/F = 2.5 \times 10^{-3} \text{ g}_{\text{cat}} \text{ min mL}^{-1}$) and the yield of acrolein was 60% (Figure S2, III–350 °C), whereas the yield for acrylic acid was 17% under this condition. To consecutively oxidize acrolein to acrylic acid over the tetragonal Mo_3VO_x catalyst, the reaction temperature and the contact time had to be increased significantly (Figure S2, III–400 °C).

The amorphous Mo_3VO_x catalyst also showed interesting behaviour concerning the selectivity to acrylic and hydrogenated products (Figure S2, IV). The conversion of allyl alcohol was lower than that of the orthorhombic Mo_3VO_x and trigonal Mo_3VO_x catalysts, but the selectivity to acrylic products (notably acrolein) was higher at 250 °C. The yields of acrylic acid were 74% at 350 °C, $W/F = 2.5 \times 10^{-3} \text{ g}_{\text{cat}} \text{ min mL}^{-1}$ and 77% at 400 °C, $W/F = 0.3 \times 10^{-3} \text{ g}_{\text{cat}} \text{ min mL}^{-1}$ over the amorphous Mo_3VO_x catalysts.

Furthermore, the consecutive oxidation to CO_x over the amorphous Mo_3VO_x was strongly limited compared to the cases over the orthorhombic Mo_3VO_x and the trigonal Mo_3VO_x catalysts. As described above, the four kinds of Mo_3VO_x catalysts have similar chemical compositions with the same layer-type structure in the c direction, whereas the arrangement of pentagonal $\{\text{Mo}_6\text{O}_{21}\}$ units in the a – b plane is different. The orthorhombic, trigonal and amorphous Mo_3VO_x catalysts are classified into similar structure-type groups that have heptagonal channels. On the other hand, the tetragonal Mo_3VO_x catalyst does not have heptagonal channels. It is known that the a – b plane of section surface and side surface of the rod-shaped crystals provide different active sites for oxidation reactions. We have found in a previous study that the heptagonal channel in a – b plane exposed by grinding treatment is far more active for selective oxidation of acrolein than is the side surface of the rod-shaped crystals by comparison with an unground catalyst.^[23] The conversion of acrolein over the unground catalyst was far less than that over the ground catalyst despite the fact that the two catalysts had almost the same external surface areas.

In the current study, the tetragonal Mo_3VO_x catalyst promoted the oxidation dehydrogenation of allyl alcohol to acrolein, but it was inactive for the oxidation of acrolein to acrylic acid. The selectivity to acrolein was 80% over the tetragonal Mo_3VO_x catalyst, implying that the section surface and/or side surface of the tetragonal Mo_3VO_x catalyst are selective for the oxidative dehydrogenation of allyl alcohol to acrolein. Because the arrangement in the c direction is identical for all four catalysts, one can assume that the differences in the catalytic performance are caused by the a – b plane. Orthorhombic and trigonal Mo_3VO_x catalysts exhibit heptagonal arrangement in

the a – b plane, which is highly active for the selective oxidation. Thus, the latter directly convert allyl alcohol to acrylic acid. However, since orthorhombic and trigonal Mo_3VO_x catalysts exhibit the same c plane as the tetragonal Mo_3VO_x one would expect to observe a competition between the reactions over the side surface and the section surface at higher reaction temperature. In Figure 5 the ratios of acrylic products (acrylic

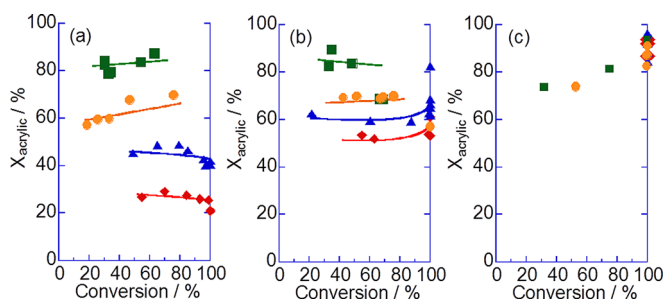


Figure 5. Effects of allyl alcohol conversion on the distribution of acrylic products at a) 250, b) 300, c) 350 °C reaction temperature over orthorhombic Mo_3VO_x (◆), trigonal Mo_3VO_x (▲), tetragonal Mo_3VO_x (■) and amorphous Mo_3VO_x (●). $X_{\text{acrylic}} = [\text{Sel. (acrylic acid)} + \text{Sel. (acrolein)}] / [\text{Sel. (acrylic acid)} + \text{Sel. (acrolein)} + \text{Sel. (propionic acid)} + \text{Sel. (propanal)}] \times 100$, reaction conditions: catalyst 25, 50, 100 mg, 2 bar, allyl alcohol/ O_2 / H_2O /(N_2 + He) = 1:2.2:42.1:11.8 (total flow rate of 20, 40, 60, 80 mL min^{-1} , see also Figure S2).

acid and acrolein) and hydrogenated products (propionic acid and propanal) over crystalline Mo_3VO_x catalysts are shown at several reaction temperatures. The distribution of acrylic products did not change regardless of the wide range of conversion, indicating that both propanal and acrolein are competitively formed on the active sites of the a – b plane surface from allyl alcohol and consecutively oxidized to propionic acid and acrylic acid, respectively (Figure 5a,b). Furthermore one can see that propionic acid was more easily oxidized to CO_2 compared to acrylic acid whereby the value of X_{acrylic} therefore increased if conversion reached 100% (Figure 5b,c). The roles of the heptagonal channel in the a – b plane have been discussed in our previous report.^[21,22,25] In the case of oxidation of small molecules such as methane and ethane, these reactants can adsorb inside of the heptagonal channel, which function as active sites. In contrast, the molecules such as propane, 2-propanol, acrolein and allyl alcohol, which cannot enter the heptagonal channel (≈ 0.4 nm in pore diameter), adsorb and interact with the open mouth of heptagonal channel. The open mouth of heptagonal would function as active sites for the oxidation.

In conclusion, the active sites for the formation of acrolein from allyl alcohol on the tetragonal Mo_3VO_x are selective but the reactivity of these active sites is not high. Therefore, acrolein formation over the tetragonal Mo_3VO_x catalysts is negligible at temperatures less than approximately 250 °C. The selective oxidation to acrylic acid is ascribed to the section surface (a – b plane). Orthorhombic and trigonal Mo_3VO_x catalysts exhibit heptagonal channel, whereby they showed almost the same behaviour for allyl alcohol oxidation. The open mouth of the heptagonal channel over the a – b plane acts as an active site

for the allyl alcohol oxidation and possesses high activity. Thus, the maximum yields in acrylic acid were 73% for the orthorhombic Mo_3VO_x catalyst and 72% for the trigonal Mo_3VO_x catalyst at 350 °C.

Conclusions

Selective oxidation of allyl alcohol was performed by using crystalline (orthorhombic, trigonal, amorphous and tetragonal) Mo_3VO_x catalysts. These four catalysts were rod-shape particles and had similar chemical compositions with the same layer-type structure in the c direction, but different arrangement of pentagonal $\{\text{Mo}_6\text{O}_{21}\}$ units in the a - b plane. The order of activity in the selective oxidation of allyl alcohol is: orthorhombic, trigonal Mo_3VO_x > amorphous Mo_3VO_x > tetragonal Mo_3VO_x . The four kinds of rod-shaped Mo_3VO_x catalysts promote the formation of acrolein from allyl alcohol commonly. However, the activity of tetragonal Mo_3VO_x was rather low whereby the acrolein formation was negligible at temperatures under approximately 250 °C. The high selective formation of acrylic acid over orthorhombic, trigonal and amorphous Mo_3VO_x catalysts was ascribed to the heptagonal channel in the a - b plane, whereby these three catalysts showed almost the same behaviour for allyl alcohol oxidation. The open mouth of the heptagonal channel over the a - b plane acts as an active site for the oxidation to acrylic acid and exhibits higher activity than the active sites in the c -plane for acrolein formation. Nevertheless, propanal and acrolein formed competitively on the active sites of heptagonal channel before they were consecutively oxidized to propionic acid and acrylic acid, respectively. Thus, the maximum yields of acrylic acid were 73% for the orthorhombic Mo_3VO_x catalyst and 72% for the trigonal Mo_3VO_x catalyst at 350 °C.

Experimental Section

Preparation of orthorhombic Mo_3VO_x mixed oxide catalyst

Orthorhombic Mo_3VO_x materials were synthesized by a hydrothermal method.^[24] $(\text{NH}_4)_6\text{Mo}_7\text{O}_{24}\cdot 4\text{H}_2\text{O}$ (Mo: 50 mmol, Wako) was dissolved in distilled water (120 mL). Separately, an aqueous solution of VOSO_4 (Mitsuwa Chemicals) was prepared by dissolving hydrated VOSO_4 (12.5 mmol) in 120 mL distilled water. These two solutions were mixed at 20 °C and stirred for 10 min before introducing them into an autoclave (300 mL Teflon inner tube). After 10 min of nitrogen bubbling to replace the residual air, hydrothermal treatment was performed at 175 °C for 48 h. The as-obtained grey solids were washed with distilled water and dried at 80 °C overnight. These solids were purified by treatment with oxalic acid; dry solids were added to an aqueous solution of oxalic acid (0.4 M; 25 mL/1 g solid) and this mixture was stirred at 60 °C for 30 min. Solids were isolated from the suspension by filtration, washed with distilled water and dried at 80 °C overnight.

Preparation of trigonal Mo_3VO_x mixed oxide

The same procedure was used for the synthesis of trigonal Mo_3VO_x , except for pH condition and duration of hydrothermal synthesis.

The pH value of the mixed solution was adjusted to 2.2 by adding sulfuric acid (2 mol L⁻¹). The hydrothermal synthesis time was 20 h.

Preparation of amorphous Mo_3VO_x mixed oxide

Mo_3VO_x material well-crystallized in the c direction but disordered in the other direction was obtained by increasing the concentration of the mixed aqueous solution, which was two-fold higher. In this paper, this material is designated as amorphous Mo_3VO_x . Other preparatory conditions were the same as those for orthorhombic Mo_3VO_x .

Preparation of tetragonal Mo_3VO_x mixed oxide

Tetragonal Mo_3VO_x was synthesized by phase transformation from orthorhombic Mo_3VO_x by heat treatment. Dried orthorhombic Mo_3VO_x was heated in air with a heating ramp of 10 °C min⁻¹ to 400 °C and kept at that temperature for 2 h before cooling to ambient temperature. The heat-treated sample was again heated in a nitrogen stream (50 mL min⁻¹) with a heating ramp of 10 °C min⁻¹ to 575 °C and kept at that temperature for 2 h.

Catalytic test for allyl alcohol selective oxidation

Allyl alcohol selective oxidation tests were performed on the REAL-CAT platform in a Flowrence high-throughput unit (Avantium) equipped with 16 parallel milli-fixed-bed reactors (internal diameter 2.6 mm, length 300 mm). Ground and calcined catalysts samples (50 mg) (673 K for 2 h under static air) were charged in each fixed-bed flow reactor and sandwiched between SiC powder (particle size: 0.21 mm, Prolabo) and heated up to reaction temperature under air flow (10 mL min⁻¹). Air was switched to reaction gas with the molar composition of allyl alcohol/ O_2 / H_2O /(N_2 + He) = 1:2.2:42.1:11.8 (total flow rate of 40 mL min⁻¹) under a pressure at 2 bar and the condition was kept for 20 min at reaction temperature. Then liquid products were collected every 140 min by trapping at 10 °C. The gas phase reactants and products after the trap system were analysed with three on-line gas chromatographs (GC) equipped as follows: Molecular Sieve (Agilent) with TCD (for O_2 , N_2 and CO), Haysep Q (Agilent) with TCD (for H_2O and CO_2), and Poraplot Q (Agilent) with FID (for organic compounds). The liquid phase reactant and products in the trap were analysed with GC-FID (ZB-WAX). The carbon balance was always more than 96%. The catalyst weight was adjusted to 0.050, 0.025 and 0.100 g and total flow rates of reactant gas were adjusted to 20, 40, 60 and 80 mL min⁻¹ with the same gas composition in order to change the contact time.

Characterization

The catalysts were characterized by the following techniques. Elemental compositions were determined by an inductive coupling plasma (ICP-AES) method (ICPE-9000, Shimadzu). Samples were dissolved in a NH_3 solution. Powder XRD patterns were measured with a diffractometer (RINT Ultima+, Rigaku) using $\text{Cu}_{\text{K}\alpha}$ radiation (tube voltage: 40 kV, tube current: 20 mA). Diffractions were recorded in the range of 4–60° with 1° min⁻¹. Catalysts used for reaction were sieved (aperture: 75 μm) to separate them from SiC. The morphology was investigated by using a scanning transmission electron microscope (HD-2000, Hitachi) at 200 kV. The samples were dispersed in ethanol by ultrasonic treatment for several minutes, and drops of the suspension were placed on a copper grid

for STEM observations. N₂ adsorption isotherms at liquid N₂ temperature were measured by using an auto adsorption system (BELSORP MAX, BEL JAPAN) for the samples. Prior to N₂ adsorption, the catalysts were evacuated under vacuum at 300 °C for 2 h. External surface area was calculated by the *t* method.

Acknowledgements

The REALCAT platform is benefiting from a Governmental subvention administrated by the French National Research Agency (ANR) within the frame of the 'Future Investments' program (PIA), with the contractual reference 'ANR-11-EQPX-0037'. The Nord-Pas-de-Calais Region and the FEDER are acknowledged for their financial contribution to the acquisition of the equipment of the platform. The Ecole Centrale de Lille and the Centrale Initiatives Foundation are also warmly acknowledged for their financial support.

Keywords: allylic compounds · hydrothermal synthesis · molybdenum · oxidation · vanadium

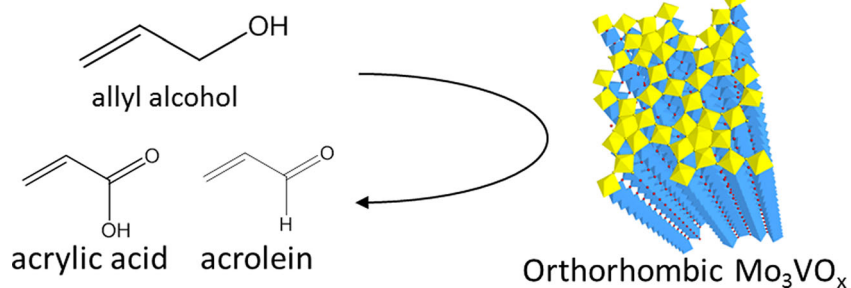
- [1] B. Katryniok, S. Paul, F. Dumeignil, *ACS Catal.* **2013**, *3*, 1819–1834.
- [2] K. Omata, S. Izumi, T. Murayama, W. Ueda, *Catal. Today* **2013**, *201*, 7–11.
- [3] A. Chierogato, M. D. Soriano, E. García-González, G. Puglia, F. Basile, P. Concepción, C. Bandinelli, J. M. López Nieto, F. Cavani, *ChemSusChem* **2015**, *8*, 398–406.
- [4] D. Sun, Y. Yamada, S. Sato, *Appl. Catal. B* **2015**, *174–175*, 13–20.
- [5] K. Omata, K. Matsumoto, T. Murayama, W. Ueda, *Chem. Lett.* **2014**, *43*, 435–437.
- [6] K. Omata, K. Matsumoto, T. Murayama, W. Ueda, *Catal. Today* **2016**, *259*, 205–212.
- [7] C. Guillon, C. Liebig, S. Paul, A.-S. Mamede, W. F. Hölderich, F. Dumeignil, B. Katryniok, *Green Chem.* **2013**, *15*, 3015.
- [8] F. Wang, J. Xu, J.-L. Dubois, W. Ueda, *ChemSusChem* **2010**, *3*, 1383–1389.
- [9] M. D. Soriano, P. Concepción, J. M. L. Nieto, F. Cavani, S. Guidetti, C. Trevisanut, *Green Chem.* **2011**, *13*, 2954–2962.
- [10] S. Thanasilp, J. W. Schwank, V. Meeyoo, S. Pengpanich, M. Hunsom, *J. Mol. Catal. A* **2013**, *380*, 49–56.
- [11] L. Shen, H. Yin, A. Wang, X. Lu, C. Zhang, *Chem. Eng. J.* **2014**, *244*, 168–177.
- [12] A. Chierogato, M. D. Soriano, F. Basile, G. Liosi, S. Zamora, P. Concepción, F. Cavani, J. M. López Nieto, *Appl. Catal. B* **2014**, *150–151*, 37–46.
- [13] L. Krähling, J. Krey, G. Jakobson, J. Grolig, L. Miksche, *Ullmann's Encyclopedia of Industrial Chemistry*, Wiley-VCH, Weinheim, **2012**.
- [14] D. F. White, US Pat. 7847135B1, **2010**.
- [15] E. Arceo, P. Marsden, R. G. Bergman, J. A. Ellman, *Chem. Commun.* **2009**, 3357–3359.
- [16] W. Bühler, E. Dinjus, H. J. Ederer, A. Kruse, C. Mas, *J. Supercrit. Fluids* **2002**, *22*, 37–53.
- [17] A. Konaka, T. Tago, T. Yoshikawa, A. Nakamura, T. Masuda, *Appl. Catal. B* **2014**, *146*, 267–273.
- [18] S. Sato, R. Takahashi, T. Sodesawa, N. Honda, H. Shimizu, *Catal. Commun.* **2003**, *4*, 77–81.
- [19] J. H. Murib, US Pat., 4051181, **1977**.
- [20] H. Kasuga, K. Matsunami, JP Pat., 2008-162907, **2006**.
- [21] S. Ishikawa, X. Yi, T. Murayama, W. Ueda, *Appl. Catal. A* **2014**, *474*, 10–17.
- [22] S. Ishikawa, X. Yi, T. Murayama, W. Ueda, *Catal. Today* **2014**, *238*, 35–40.
- [23] C. Qiu, C. Chen, S. Ishikawa, T. Murayama, W. Ueda, *Top. Catal.* **2014**, *57*, 1163–1170.
- [24] T. Konya, T. Katou, T. Murayama, S. Ishikawa, M. Sadakane, D. Buttrey, W. Ueda, *Catal. Sci. Technol.* **2013**, *3*, 380–387.
- [25] S. Ishikawa, D. Kobayashi, T. Konya, S. Ohmura, T. Murayama, N. Yasuda, M. Sadakane, W. Ueda, *J. Phys. Chem. C* **2015**, *119*, 7195–7206.

Received: April 13, 2016

Revised: May 10, 2016

Published online on ■ ■ ■ ■, 0000

FULL PAPERS



Channels required: The catalytic oxidation of allyl alcohol over orthorhombic, trigonal, tetragonal, and amorphous Mo_3VO_x catalysts was investigated. Acrylic acid was formed effectively over

orthorhombic, trigonal, and amorphous Mo_3VO_x catalysts, with conversion of allyl alcohol to acrolein taking place at the heptagonal channel mouths.

T. Murayama, B. Katryniok, S. Heyte, M. Araque, S. Ishikawa, F. Dumeignil, S. Paul, W. Ueda*



Role of Crystalline Structure in Allyl Alcohol Selective Oxidation over Mo_3VO_x Complex Metal Oxide Catalysts

